ОБЪЕДИНЕННЫЙ
ИНСТИТУТ
ЯДЕРНЫХ
ИССЛЕДОВАНИЙ
ДУБНА

E7-82-46

C.Borcea, E.Gierlik, A.M.Kalinin,
R.Kalpakchieva, Yu.Ts.Oganessian, T.Pawlat,
Yu.E.Penionzhkevich, A.V.Rykhlyuk

EMISSION OF HIGH-ENERGY CHARGED PARTICLES AT 0° IN Ne-INDUCED REACTIONS

Submitted to "Nuclear Physics"

1982

Борча К. и др. E7-82-46
Эмиссия высокоэнергетических заряженных частиц под углом 0°
в реакциях с ионами неона

Измерялись инклюзивные энергетические спектры легких заряженных частиц, образующихся при бомбардировке мишеней из ^{232}Th, ^{181}Ta, ^{ест}Ti и ^{12}C ионами ^{22}Ne с энергией 178 МэВ и ^{ест}Ti ионами ^{20}Ne с энергией 196 МэВ. Продукты реакции анализировались и регистрировались $\Delta E-E$ телескопом, находящимся в фокальной плоскости магнитного спектрометра, расположенного под углом 0°. Во всех изученных реакциях с относительно большой вероятностью испускались легкие заряженные частицы с энергией, близкой к соответствующему кинематическому пределу для двухтельного выходного канала. Полученные результаты позволяют сделать выводы относительно механизма испускания легких заряженных частиц.

Работа выполнена в Лаборатории ядерных реакций ОИЯИ.

Препринт Объединенного института ядерных исследований. Дубна 1982

Borcea C. et al. E7-82-46
Emission of High-Energy Charged Particles at 0°
in Ne-Induced Reactions

Inclusive energy spectra have been measured for light charged particles emitted in the bombardment of ^{232}Th, ^{181}Ta, ^{nat}Ti and ^{12}C targets by ^{22}Ne ions at 178 MeV and a ^{nat}Ti target by ^{20}Ne ions at 196 MeV. The reaction products were analysed and detected by means of a $\Delta E-E$ telescope placed in the focal plane of a magnetic spectrometer located at an angle of 0° with respect to the beam direction. In all the reactions studied light charged particles with an energy close to the respective calculated kinematic limit for a two-body exit channel are produced with relatively great probability. The results obtained make it possible to draw some conclusions about the reaction mechanism involving the emission of light charged particles.

The investigation has been performed at the Laboratory of Nuclear Reactions, JINR.

Preprint of the Joint Institute for Nuclear Research. Dubna 1982

In heavy ion reactions light charged particles are emitted with cross sections which, particularly in the case of α-particles, constitute a significant part of the geometrical cross section of the reaction [1-5]. The measured energy spectra, angular distributions and cross sections of these particles are not describable in the framework of the evaporation model of compound nucleus decay. The noticeable increase in the yields of energetic light particles, as well as their strongly forward-peaked angular distributions suggest a fast mechanism of their formation [5,6]. The experimental investigation of p-, d-, t- and α-particle spectra as a function of the momentum transfer, reported in ref. [7] convincingly shows that the emission of fast particles takes place during the early stages of the reaction, when the final fate of the interacting nuclei is yet not determined.

Lately different theoretical models to interpret the emission mechanism of light fast particles in heavy-ion reactions have been developed [8-14]. However, an unambiguous interpretation of the process has not so far been given.

Of great interest from the point of view of understanding the mechanism of the reactions involving fast particle emission, there seems to be the experimental investigation of the energy spectra of these particles in the region of their kinematic limit, i.e., in the region of the maximum possible energy for a given reaction, estimated on the basis of conservation laws. Earlier we carried out some experiments to study the limiting energies of α-particles in different reactions [16,15]. The results obtained indicate that in heavy ion reactions α-particles with an energy close to the kinematic limit for a two-body exit channel are formed with great probability. It has been shown [16,17] that in this case a "cold" nucleus is formed whose mass is by 4 units and atomic number by 2 units smaller than those of the compound nucleus. Such a residual nucleus, formed after the emission of a high-energy α-particle may possess a significant rotational energy [18].

The experiments described in the present paper are an extension of our earlier studies [6,15] and were carried out in order to measure the probability of emission of other more complex charged particles, as well as protons, with energies close to the kinematic limit at an angle of 0° with respect to the beam direction.

EXPERIMENTAL ARRANGEMENT

The experiments were performed on external beams from the 300 cm heavy ion cyclotron of the JINR Laboratory of Nuclear Reactions. Self-supporting targets of ^{nat}Ti , ^{181}Ta and ^{232}Th were bombarded by ^{22}Ne and ^{20}Ne ions at 178 and 196 MeV, respectively. The energy resolution of the ion beam was better than 1%. The detection and analysis of reaction products were carried out with the help of a magnetic spectrometer of type MSP-144, located at an angle $\theta = 0°$ with respect to the beam direction and having an angular aperture $\theta = \pm 2°$. The energy resolution of the spectrometer was $dE/E \approx 5 \times 10^{-4}$ in a wide range of momenta $(P_{max}/P_{min} \approx 2.6)$ /19/. In the focal plane of the spectrometer a telescope of two semiconductor detectors was placed. For different purposes, the thickness of the ΔE-detectors was varied from 50 μm to 550 μm. The E-detector was 3.5 mm thick. At the maximum magnetic rigidity of the spectrometer field the energy of α-particles detected by the ΔE–E telescope was 120 MeV. The corresponding energy of other charged particles was 120 Z_i^2/A, Z_i being the effective charge and A the mass number of the particle. In those experiments in which charged particles of higher energy were detected, in order to degrade their energy a thick absorber was placed in front of the magnetic spectrometer entrance. This absorber was made of the same material as the target itself. It also served to absorb the beam. The width of the ΔE–E telescope in the focal plane corresponded to an energy interval of the order of 1%. Using this setup we could unambiguously identify light charged particles with $1 \leq Z \leq 4$ (p, d, t, ^3He, ^4He, ^6He, ^8He, ^6Li , ^7Li , ^8Li , ^7Be , ^9Be, ^{10}Be). For normalization purposes, the beam was monitored by means of a surface-barrier detector placed at 30° with respect to the incident beam.

EXPERIMENTAL RESULTS

The energy spectra of the He and H isotopes produced in the bombardment of a ^{232}Th target by ^{22}Ne ions at 178 MeV are shown in Fig.1. The full lines are drawn through the experimental points to guide the eye. The arrows on the E_{lab}-axis indicate the limiting values of the particle energies (specified for different particles by their mass numbers), calculated on the basis of the energy and momentum conservation laws under the assumption of two-body kinematics. These energy limits were estimated with an accuracy corresponding to the accuracy of determining both the heavy ion beam energy and the reaction Q value /20/, and amounting to about 2 MeV.

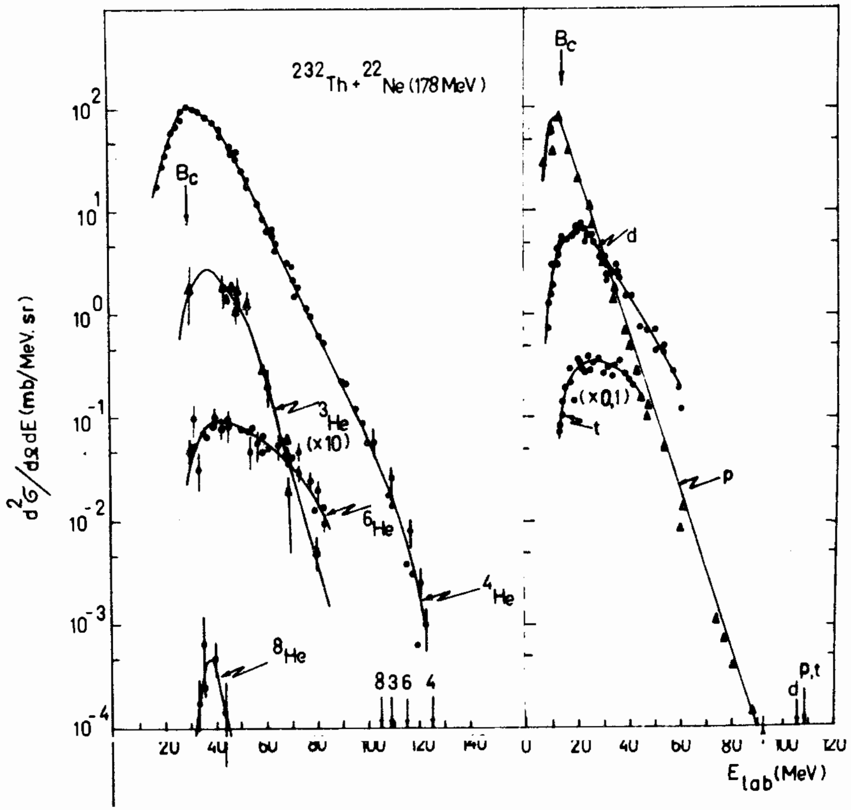

Fig.1. Energy spectra of light particles with Z=1 and 2, measured in the ^{232}Th + ^{22}Ne (178 MeV) reaction. The arrows on the E_{lab} axis indicate the calculated end-point energies for the corresponding isotope in the case of a two-body exit channel.

As is seen from the figure, in the case of α-particles, an experimental energy limit was obtained, which turned out to be ~3 MeV lower than the calculated one. The proton energy spectrum was measured up to E_p = 90 MeV, where the cross section decreases by about six orders of magnitude compared to the cross section in the spectrum maximum. The magnetic rigidity of the spectrometer made it impossible to measure the higher parts of the deuteron, triton and ^6He-spectra.

Figure 2 shows the energy spectra of Li and Be isotopes obtained in the same reaction $^{232}Th + ^{22}Ne$ (178 MeV). As is

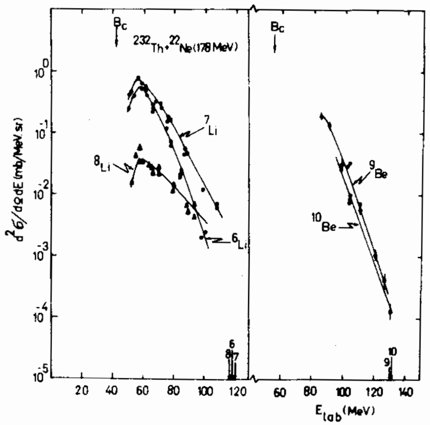

Fig.2. Same as in Fig.1, for the Li and Be isotopes.

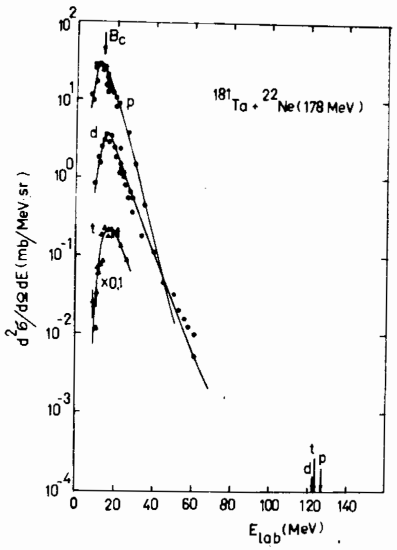

Fig.3. Energy spectra of protons, deuterons and tritons, obtained in the $^{181}Ta + ^{22}Ne$ (178 MeV) reaction.

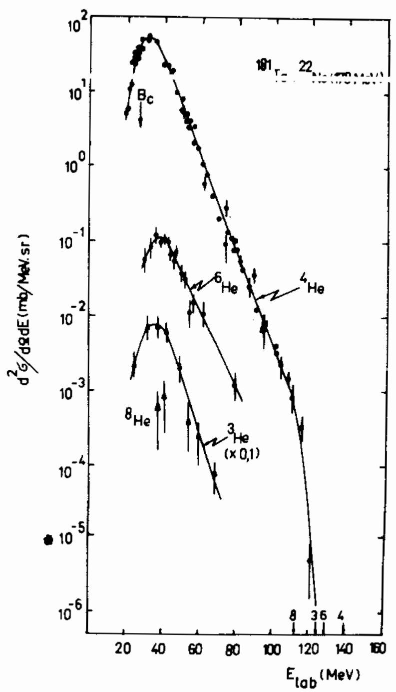

Fig.4. Same as in Fig.3, for the He isotopes.

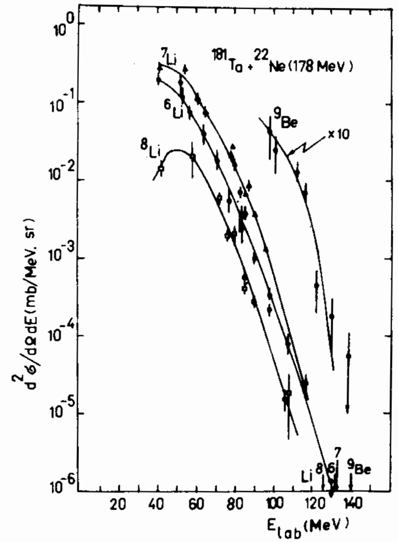

Fig.5. Same as in Fig.3, for the Li isotopes and ^9Be.

seen from this figure, practically all particles reach their kinematic energy limits with cross sections of the order of 10^{-3} - 10^{-4} mb (MeV.sr)$^{-1}$.

The energy spectra of light charged particles with Z=1,2,3, and 4, emitted in the bombardment of a ^{181}Ta target by ^{22}Ne ions at 178 MeV, are displayed in Figs.3,4 and 5. Our attention is drawn by the sharp cut-off of the α-particle spectrum near the kinematic limit (Fig.4), and also by an increase in the gap between the experimental spectrum end-point and the calculated one, in comparison with the α-particle spectrum in the case of the $^{232}Th + ^{22}Ne$ reaction (Fig.1). At an α-particle energy of 126 MeV, which is about 13 MeV below the calculated kinematic limit (see Fig.4), we did not observe a single α-particle at a cross section level of 5×10^{-7} mb (MeV.sr)$^{-1}$.

Figure 6 shows the energy spectra of He isotopes measured in the irradiation of a ^{nat}Ti target with 178 MeV ^{22}Ne ions. The energy spectra of the isotopes of He, Li and Be, displayed in Figs.7 and 8, have been obtained in the bombardment of a ^{nat}Ti target with ^{20}Ne ions at 196 MeV. For the last two figures the calculated kinematic limits are given in Table 2. It should be noted that, despite the difference in mass and energy of the projectiles (178 MeV ^{22}Ne and 196 MeV ^{20}Ne ions), the energy spectra of the light particles produced in reactions with the ^{nat}Ti target show practically no difference.

In Tables 1 and 2 there are brought together the characteristic parameters in the c.m. system of the measured spectra - the positions of the maxima of the distributions ($E_{m.p.}$), the full widths at half maximum (FWHM), the effective temperature (T_{eff}), the cross section ($d\sigma/d\Omega$), and the calculated kinematic energy limits (E^{calc}_{lim}). The effective temperature T_{eff} was estimated using the assumption of the Maxwellian form of the spectrum, i.e.,

$$\frac{d^2\sigma}{d\Omega\, dE} \sim (E - B_c) \exp\left(- \frac{E - B_c}{T_{eff}}\right),$$

where B_c is the c.m. exit channel Coulomb barrier.

As is seen from the Tables, the effective temperature increases both with the target mass and the mass of the emitted particle (an exception is the ^8He-spectrum). Assuming that the temperature is related to the reaction time, the increasing temperature with the mass of the emitted particle, in our opinion, means that the more complex particles are emitted during the earlier stages of the reaction evolution.

Table 1

Characteristic parameters of light particle spectra for the reactions $^{181}Ta + ^{22}Ne$ and $^{232}Th + ^{22}Ne$

Particle	$^{181}Ta + ^{22}Ne$ (178 MeV)						$^{232}Th + ^{22}Ne$ (178 MeV)					
	$E_{m.p.}$	B_c	FWHM	T_{eff}	$d\sigma/d\Omega$	E^{calc}_{lim}	$E_{m.p.}$	B_c	FWHM	T_{eff}	$d\sigma/d\Omega$	E^{calc}_{lim}
p	10	11.5	7	4.0	238	120.3	11	13	7	4.8	705	103.3
d	12.5	11.0	8	4.9	33	113.3	16	12.5	18	7.7	138	98.3
t	13.5	10.8	~10.5	5.4	~21	112.1	21	12.3	25		~110	99.4
^3He	29.5	21.3	16	4.7	1.2	112.7		24.3	19	4.5	4.8	99.8
^4He	25	21.0	13	5.6	725	125.2	26.5	23.9	18	7.1	2050	114.6
^6He	28.5	20.4	14	7.1	1.7	110.9	35	23.2	29	12.8	2.7	102.7
^8He		19.9				94.6	29.5	22.8	6	3.3	0.0043	91.3
^6Li		30.2		5.7*		115.4	49	34.4	14	5.9	7.9	105.0
^7Li		29.8		5.8*		115.1	47	34.1	17	8.1	11.1	106.6
^8Li		29.5		5.1*		107.9	48	33.8	20	10.7	0.7	101.7
^9Be		38.6		7.0*		117.6		44.2		5.1		113.5
^{10}Be								43.9		5.5		114.3

* - T_{eff} is estimated for the energy range 70-110 MeV; $E_{m.p.}$ is the most probable energy of the light particle (in MeV); B_c is the exit Coulomb barrier in MeV; FWHM and T_{eff} are the full width at half-maximum of the energy spectra and the effective temperature in MeV, respectively; $d\sigma/d\Omega$ is the differential cross section for particle production in mb/sr; $E^{calc.}_{lim}$ is the calculated kinematic limit (in MeV) for a two-body exit channel. All the quantities are given in the c.m. system.

Table 2

Characteristic parameters of the light particle energy spectra in the reactions $^{nat}Ti + ^{22}Ne$ and $^{nat}Ti + ^{20}Ne$

Particle	$^{nat}Ti + ^{22}Ne$ (178 MeV)						$^{nat}Ti + ^{20}Ne$ (196 MeV)					
	$E_{m.p.}$	B_c	FWHM	T_{eff}	$d\sigma/d\Omega$	E^{calc}_{lim}	$E_{m.p.}$	B_c	FWHM	T_{eff}	$d\sigma/d\Omega$	E^{calc}_{lim}
^3He		10.5		4.3		113.4	16.5	10.5	15	4.3	4.4	127.9
^4He	13	10.2	13	4.8	738	124.5	14	10.3	14	5.2	510	137.8
^6He	17.5	9.9	16	5.9	1.2	104.2	20	10.0	18	5.1	0.3	115.2
^8He	16.5	9.7	7.5	3.5	~0.0062	84.2		9.7		2.5		93.0
^6Li	20	14.4		4.0		106.9	24.5	14.5	15	4.2	3.5	119.9
^7Li	24.5	14.2		4.5		104.6	25	14.3	16	4.8	2.6	116.5
^8Li	25	14.0		5.0		95.1	25	14.1	18	4.8	0.17	106.1
^9Be	31	17.9		3.0		103.2		18.0		4.0		115.1
^{10}Be	31	17.7		4.3		100.6	36	17.8		4.1		111.2

The notations are the same as in Table 1.

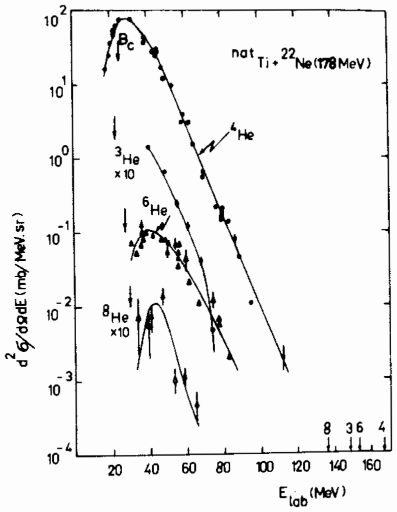

Fig.6. Energy spectra of the He isotopes, measured in the $^{nat}Ti + ^{22}Ne$ (178 MeV) reaction.

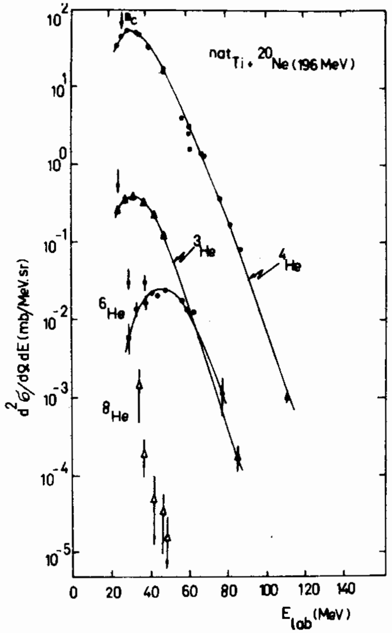

Fig.7. Energy spectra of the He isotopes, measured in the $^{nat}Ti + ^{20}Ne$ (196 MeV) reaction.

DISCUSSION

From the results shown in Figs.1-8 and Tables 1 and 2 it follows that the spectra of all light particles emitted at 0° with respect to the beam, as in the case of α-particles /6/, have their maxima several MeV above the exit Coulomb barrier and tend to exponentially fall to some limiting energy determined by the conservation laws for a given reaction channel. The measurement of the energy spectrum of the emitted particles in the region of the kinematic limit, in our opinion, allows one to make some conclusions about their formation mechanism as the kinematic limit itself depends on the masses and the number of particles in the exit channel. To illustrate this we shall consider a reaction involving the emission of ^4He in the interaction of ^{22}Ne ions with ^{181}Ta nuclei (Fig.4). Several mechanisms can be assumed to govern the emission of α-particles in this reaction, namely:

(1) At the moment of α-particle formation in the exit channel there are only two nuclei: $^{181}Ta + ^{22}Ne \rightarrow ^4He + ^{199}Tl$. In this case we are not interested in the further fate of the heavy residual - its deexcitation.

(2) The breakup of the ^{22}Ne nucleus into an α-particle and ^{18}O at the moment of interaction with the ^{181}Ta nucleus, i.e., $^{181}Ta + ^{22}Ne \rightarrow \alpha + ^{18}O + ^{181}Ta$.

(3) The knockout of an α-particle from the target nucleus: $^{181}Ta + ^{22}Ne \rightarrow \alpha + ^{22}Ne + ^{177}Lu$.

(4) and (5). Symmetric and asymmetric fission involving the simultaneous emission of an α-particle:

$$^{181}Ta + ^{22}Ne \rightarrow ^{128}_{50}Sn + ^{71}_{31}Ga + \alpha \quad \text{and} \quad ^{98}_{40}Zr + ^{101}_{41}Nb + \alpha.$$

(6) The emission of an α-particle by one of the fission fragments of the compound nucleus:

$$^{181}Ta + ^{22}Ne \rightarrow ^{98}_{40}Zr + ^{105}_{43}Tc$$
$$\downarrow$$
$$\alpha + ^{94}_{38}Sr \; .$$

For all the reactions mentioned it is possible to calculate the maximum possible energy available for the α-particle: in the first case this energy is calculated as for two-body kinematics /21/. In all other cases the maximum possible energy was calculated using the prescription of Ohlsen /22/. In these cases it is necessary to take into account the presence of three charged particles in the exit channel. Their Coulomb interaction leads to a decrease in the total energy E_c^{tot} (in the c.m. system). According to eqs. (20) and (21) from ref. /22/ the energy balance for a three-body reaction can be written as follows:

$$E_{1-23} + E_{23} = E_c^{tot} = Q + m_t E_p^{\ell}/(m_p + m_t) \; ,$$

$$E_{1-23} = ME_1^c/(m_2 + m_3).$$

Hence

$$E_1^c = \frac{m_2 + m_3}{M}(E_c^{tot} - E_{23}) \; ,$$

where E_1^c is the possible energy for a definite nucleus in the c.m. system, $M = m_1 + m_2 + m_3$, m_i being the mass number of the particle, and E_{23}^* is the excitation energy of particles 2 and 3. The quantity E_1^c attains the maximum possible value solely at the minimum value of E_{23}, i.e., at zero excitation of the remaining nuclei. However, in the case of three charged particles in the exit channel it is necessary to take into account the Coulomb repulsion between them, V_{23}^c. Then

$$E_{1,max}^c = \frac{m_2 + m_3}{M}(E_c^{tot} - V_{23}^c).$$

The maximum possible energies (calculated in MeV) of α-particles produced in any of the above six cases are given in Table 3.

Table 3

Calculated kinematic limits for different α-particle emission mechanisms in the interaction of ^{22}Ne(178 MeV) with ^{181}Ta

Reaction	(1)	(2)	(3)	(4)	(5)	(6)
Q	-31.013	-9.663	1.535	94.66	111	
V^c_{23}		70.5	84.3	168.8	179.5	
$E^{cm}_{\alpha,max}$	125.2	76.9	74.4	82.9	88.4	
$E^{lab}_{\alpha,max}$	139.3	88.1	85.4	94.5	100.4	~60

In the case of evaporation of an α-particle from a fission fragments (column 6) its maximum energy was determined taking into account the average kinetic energy (E^{lab}_{Zr}=70 MeV) and maximum excitation ($E^*_{Zr,max}$= 63 MeV) of the fragment, by using the following expression

$$E^{lab}_{Zr} \cdot \frac{m_\alpha}{m_{Zr}} + E^*_{Zr,max} + Q_\alpha \approx 60 \text{ MeV},$$

where Q_α (-4.76 MeV) is the α-particle binding energy in the Zr nucleus. From Table 3 one can clearly see that the formation of α-particles with energies >100 MeV is forbidden in all three-body processes, this being possible only in the case of a two-body one (1). Comparing our calculations with the experimental data (Fig.4) we can state that at α-particle energies above 100 MeV the final channel of the reaction involves only the ^4He and the ^{199}Tl nuclei. This fact makes it possible to assume that the deviation of the α-particle energy spectrum from the exponential fall at energies above 115 MeV is due to populating an yrast band in the Tl nucleus. This can also account for the gap between the calculated end-point of the spectrum (139 MeV) and the experimental one (122 MeV). In the case of the reaction under consideration (^{22}Ne+Ta) the angular momentum value calculated for grazing collision is equal to ℓ_{gr} = 98ħ(ref./23/). Assuming the emission of an α-particle with maximum energy during the inverse grazing process, we obtain the value of angular momentum carried off by the α-particle, ℓ=49ħ. Angular momentum $\ell\approx$50ħ remains in

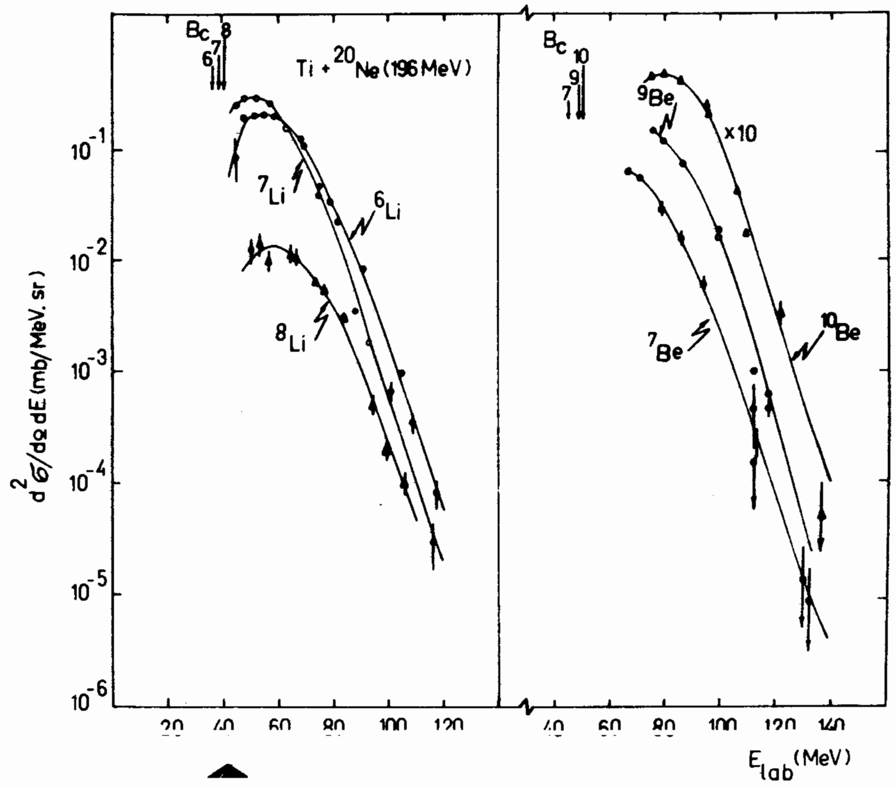

Fig.8. Same as in Fig.7, for the Li and Be isotopes.

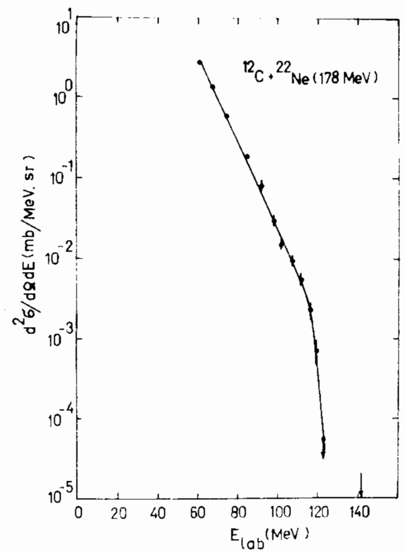

Fig.9. The α-particle energy spectrum measured in the ^{12}C+^{22}Ne (178 MeV) reaction.

the Tl nucleus. Considering a two-body mechanism it is possible to obtain the rotational energy of the remaining nucleus, about 13 MeV. This value agrees well with the above-mentioned difference between the calculated maximum possible and experimental end-point energies. Similar calculations can be carried out for the Ne + Th system (Fig.2), in which the final nucleus is heavier than that in the previous case and the moment of inertia is larger. As observed experimentally, the rotational energy in this case is small (~2 MeV). On the contrary, at a small moment of inertia, as is the case in the interaction of ^{22}Ne projectiles with the ^{12}C nuclei, this difference between the calculated and experimental end-point energies reaches 20 MeV (Fig.9). However it is necessary to note that in this combination there may be a large contribution of the three-body process in which the ^{12}C nucleus breaks up into 3α-particles, one of them being captured by the ^{22}Ne ion. On the other hand, in the case of emission of heavy fast particles (^{9}Be, ^{10}Be) in the interaction of Ne ions with heavy nuclei the maximum energy of the Be nuclei practically reaches the kinematic limit, i.e., the residue left after the emission of the Be nucleus is practically "cold", having small rotational energy. This fact may prove rather essential for the production of new heavy and superheavy nuclei.

There are presently a great many theoretical models elaborated in attempts to interpret experimental results on light charged particle emission in heavy ion reactions [14,24-26]. All of these models were confronted to the evaporation model of compound-nucleus decay [27]. However, one of the recent papers by Blann [28] deals with calculations taking into account the dependences of the penetrability coefficients on the deformation and angular momenta of the nuclei. These calculations have demonstrated that at large angular momenta the probability of charged particle emission increases considerably and the emission of charged clusters becomes stronger at large deformations of the compound nucleus. This approach, however, does not provide the possibility of explaining the high effective temperature extracted from experimental cross sections, and the relatively large yield of high-energy charged particles.

The authors of paper [13] make an attempt to interpret the high effective temperature, observed experimentally in terms of the existence of several components in the spectrum of the particles observed. In particular, they discriminate between the evaporation component and another, fast one which is interpreted within the framework of the "hot spot" model. The authors of that paper [13] compared their calculations with the

results of our earlier study of α-particle emission [6] and obtained a fairly good agreement in the slopes of the spectra. At present the "hot spot" model is developed by many authors from a microscopic point of view [11,29-31]. Macroscopically, this model interprets the source of particle emission as a strong local excitation at the point of contact between the two interacting nuclei with the simultaneous rotation of the system formed [32,33]. The "hot spot" moves into the nucleus while a total energy transfer from the incident ion takes place. The evaporation of any particle is admissible at each stage of this evolution. To elucidate the energy spectra of light charged particles the "rotating hot spot" model suggested in paper [32] assumes that the spot of local heating moves with approximately half the beam velocity. The formula for the production cross section derived in ref. [33] describes with good accuracy most of the energy spectra measured by us, except those of ^{3}He and ^{8}He, and those spectra parts lying near the kinematic limit. A formula for the temperature of the moving spot is given in the same paper [33]. The calculations carried out by this formula have given values close to the experimental ones listed in Tables 1 and 2. This formula reflects the experimentally established fact of an increase in temperature with the increasing mass of the target nucleus but it neglects the dependence on the particle mass in the exit channel. We believe that it is possible to obtain, within the framework of the model being discussed, a decrease in the spectrum slope (the temperature growth) with increasing isotopic mass if a time dependence of the velocity of the moving source is introduced.

In our opinion, the direct reaction model may prove advantageous for explaining the spectra shapes and light-particle formation cross sections near the kinematic limit. In papers [25,34,35] this approach has already been employed to describe the shapes of the light charged particle spectra measured in heavy ion reactions - the direct reaction was considered as a breakup of the projectile into two parts one of which is absorbed by the target nucleus. In view of the fact that earlier we obtained a sharp dependence of the formation cross section of high energy charged particles upon their binding energy in the target nucleus [6], this process can be interpreted as the knock-out of a particle by the incident ion. V.Bunakov et al. [34] are presently elaborating this approach and have obtained a qualitative explanation of the α-particle spectrum shape even in the vicinity of the kinematic limit, as well as the dependence of the cross section for forming high-energy α-particles on their binding energy in the target nucleus. Unfortunately, these calculations are so far of qualitative character since more accurate data on some parameters including the spectroscopic factors of light particles, are needed. In our view, the development of this approach can contribute to the interpretation of the reactions involving the emission of high-energy light particles.

From the data obtained in the present paper we can draw the following conclusions.

(1) In all the reactions we have investigated, high-energy light charged particles (p , d , t , ^{3}He, ^{4}He, ^{6}He , ^{6}Li , ^{7}Li , ^{8}Li , ^{7}Be , ^{9}Be , ^{10}Be) are produced with relatively large cross sections and energies that are close to the reaction kinematic limit calculated assuming a two-body exit channel.

(2) The end-point energy of the energy spectra of light charged particles (except ^{3}He and ^{8}He) is only 5-10 MeV below the kinematic limit for the given reaction, this difference decreasing with the increasing masses of the particle emitted and the target nucleus. The latter fact can serve as evidence that pure rotational levels are excited at zero excitation thermal energy in the remaining nucleus.

(3) The effective temperature determined by the slopes of the energy spectra increases with the mass of the particle emitted. This may indicate that more exotic particles are emitted at an earlier stage of the reaction.

In conclusion the authors would like to express their gratitude to Academician G.N.Flerov for his interest in the present study, and to V.E.Bunakov, R.V.Jolos, B.I.Pustylnik and Yu.A.Muzychka for useful discussions. Thanks are also due to Z.D.Pokrovskaya and A.Belozyorov for their assistance in performing the experiments, Yu.P.Kharitonov and V.F.Kushniruk for manufacturing the semiconductor detectors.

REFERENCES

1. Britt H.C., Quinton A.R. Phys.Rev., 1961, 124, p.877.
2. Kapuscik A. et al. Yad.Fiz., 1967, 6, p.1142.
3. Galin J. et al. Phys.Rev., 1974, C9, p.1126.
4. Volkov V.V. et al. Izv.AN SSSR, ser.fiz., 1978, 42, p.2234.
5. Gierlik E. et al. Yad.Fiz., 1980, 32, p.45.
6. Borcea C. et al. Nucl.Phys., 1981, A351, p.312.
7. Awes T.C. et al. Phys.Lett., 1979, 87B, p.43.

8. Blann M., Mignerey A., Scobel W. Nukleonika, 1976, 21, p.335.
9. Zolnowsky D.R. et al. Phys.Rev.Lett., 1978, 41, p.92.
10. Wilczynski J. et al. Phys.Rev.Lett., 1980, 45, p.606.
11. Weiner R., Weström M. Nucl.Phys., 1977, A286, p.282.
12. Garpman S.I.A., Sperber D., Zielinska-Pfabe M. Phys. Lett., 1980, B90, p.53.
13. Jolos R.V., Ivanona S.P., Kartavenko V.G. JINR, P4-81-238, Dubna, 1981.
14. Karvinen A.O.T., De J.N., Jakobsson B. Nucl.Phys., 1981, A367, p.122.
15. Gierlik E. et al. Z.Phys., 1980, A295, p.295.
16. Borcea C. et al. Izv. AN SSSR, ser.fiz., 1980, 44, p.2234.
17. Bruchertseifer H. et al. Yad.Fiz., 1981, 33, p.1453.
18. Oganessian Yu.Ts. Proc. Int.School on Nucl.Phys., Alushta, April 14-25, 1980. JINR, D4-80-385, Dubna, 1980, p.261.
19. Maidikov V.Z. et al. JINR, P7-81-140, Dubna, 1981.
20. Takahashi K., Groote H.V., Hilf E.R. IKDA 76/26, Darmstadt, 1976.
21. Marion J.B., Young F.C. Nuclear Reaction Analysis. Graphs and Tables. North-Holland, Amsterdam, 1968.
22. Ohlsen C. Nucl.Instr.Meth., 1965, 37, p.240.
23. Nörenberg W., Weidenmüller H.A. Lecture Notes in Physics, Springer Verlag, 1976.
24. Bondorf J.P. et al. Phys.Lett., 1979, 84B, p.162.
25. Inamura T. et al. Phys.Lett., 1979, 84B, p.71.
26. Wu J.R., Lee I.Y. Phys.Rev.Lett., 1980, 45, p.8.
27. Ericson T. Adv.Phys., 1960, 9, p.425.
28. Blann M., Komoto T.T. Phys.Rev., 1981, C24, p.426.
29. Gottschalk P.A., Weström M. Phys.Rev.Lett., 1977, 39, p.1250.
30. Morison W.W. et al. Phys.Lett., 1980, 93B, p.379.
31. Jolos R.V., Kartavenko V.G. JINR, P4-80-37, Dubna, 1980.
32. Awes T.C. et al. Phys.Lett., 1981, 103B, p.417.
33. Awes T.C. et al. Phys.Rev., 1981, C24, p.89.
34. Bunakov V.E., Zagrebayev V.I. Preprint Leningrad Inst. of Nucl. Phys., No.650, 1981.
35. Lukyanov V.K., Petkov I. Nucl.Phys., 1963, 49, p.529.

Received by Publishing Department
on January 21 1982.

SUBJECT CATEGORIES OF THE JINR PUBLICATIONS

Index	Subject
1.	High energy experimental physics
2.	High energy theoretical physics
3.	Low energy experimental physics
4.	Low energy theoretical physics
5.	Mathematics
6.	Nuclear spectroscopy and radiochemistry
7.	Heavy ion physics
8.	Cryogenics
9.	Accelerators
10.	Automatization of data processing
11.	Computing mathematics and technique
12.	Chemistry
13.	Experimental techniques and methods
14.	Solid state physics. Liquids
15.	Experimental physics of nuclear reactions at low energies
16.	Health physics. Shieldings
17.	Theory of condenced matter
18.	Applied researches
19.	Biophysics